Angle measures for an MPT characterisation of a computed toy gun

26th March 2024

Barrel has $\sigma_* = 1.45 \times 10^6$ S/m and μ_r is varied ($\mu_r = 100$ corresponds to carbon steel) and the receiver has 4.5×10^6 S/m and $\mu_r = 1$ and is a stainless steel. The barrel is hollow with a cap at one end. The length of the barrel is 0.2 m, outer and inner radii of the barrel are 0.02 m and 0.01m, respectively. The box representing the receiver is 0.08 m $\times$ 0.01 m $\times$ 0.15 m. A mesh of 21,132 unstructured tetrahedra, 5,525 prisms and elements of order $p = 0, 1, 2, 3, 4, 5$ are considered. The prisms are chosen to be used as boundary layers in the barrel, which has a smaller skin depth.

Figure 1: Illustration of the toy gun. Barrel has $\sigma_* = 1.45 \times 10^6$ S/m and μ_r is varied ($\mu_r = 100$ corresponds to carbon steel) and the receiver has 4.5×10^6 S/m and μ_r and is a non-magnetic stainless steel.

When the eigenvalue curves cross each other then this indicates the presence of eigenvalues with algebraic multiplicity greater than one. The associated eigenvectors for an eigenvalue with algebraic multiplicity two can be arbitrarily chosen as any two vectors that form a basis for the two-dimensional eigenspace. In numerical computations, the computation of eigenvectors associated with eigenvalues λ_n, λ_m is problematic when $\lambda_n \to \lambda_m$.

Angles between the computed eigenvectors using the metrics d_R and d_F are considered and the approximations d_E and d_C that do not require knowledge of the eigenvectors. Notice the smooth transition of d_R and d_F in the regions where the eigenvalues are repeated and the associated **peaks**. While we know there are issues with the eigenvectors of repeated eigenvalues, the peaks are interesting as there is a **smooth transition to them**. While d_E and d_C do not capture the peaks well, particularly d_E, the normalising constant involved in the computation do identify the peaks.

Note that d_E and d_C do capture the behaviour of d_R and d_F well for other objects when there are no peaks.

0.1 Barrel with $\mu_r = 20$

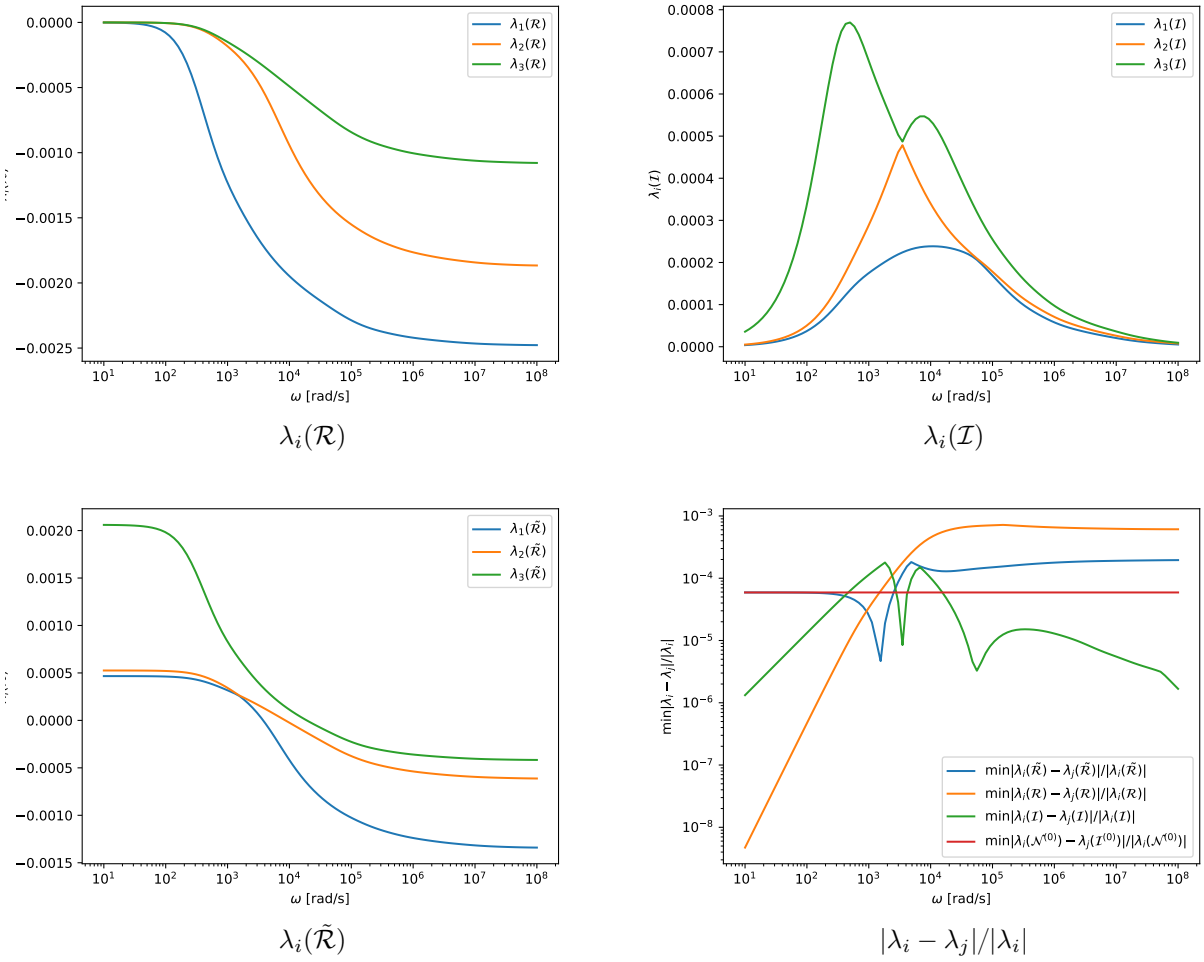

Figure 2: Computed eigenvalue spectral signatures and eigenvalue proximity for the toy gun with $\mu_r = 20$ in the barrel.

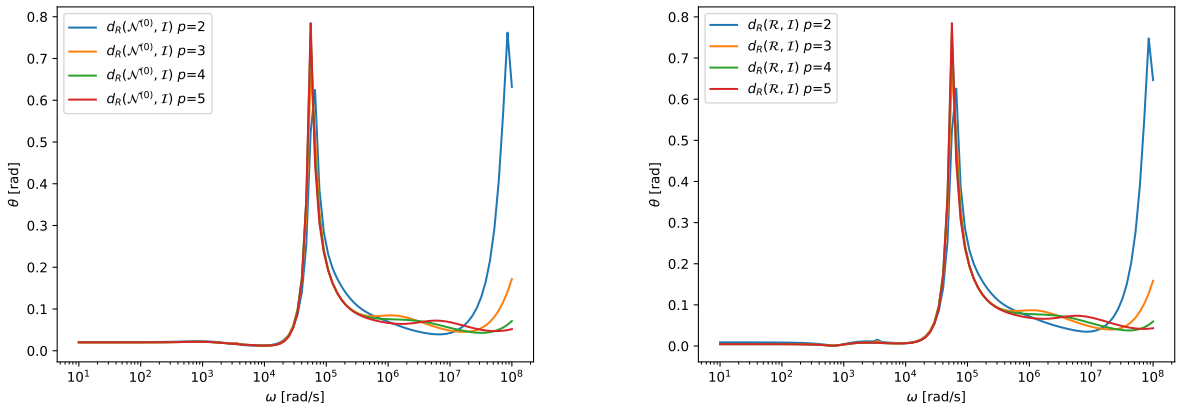

Figure 3: Examples of p refinement for the toy gun with $\mu_r = 20$ in the barrel. Angle measures $d_R(\mathcal{N}^{(0)}, \mathcal{I})$ and $d_R(\mathcal{R}, \mathcal{I})$

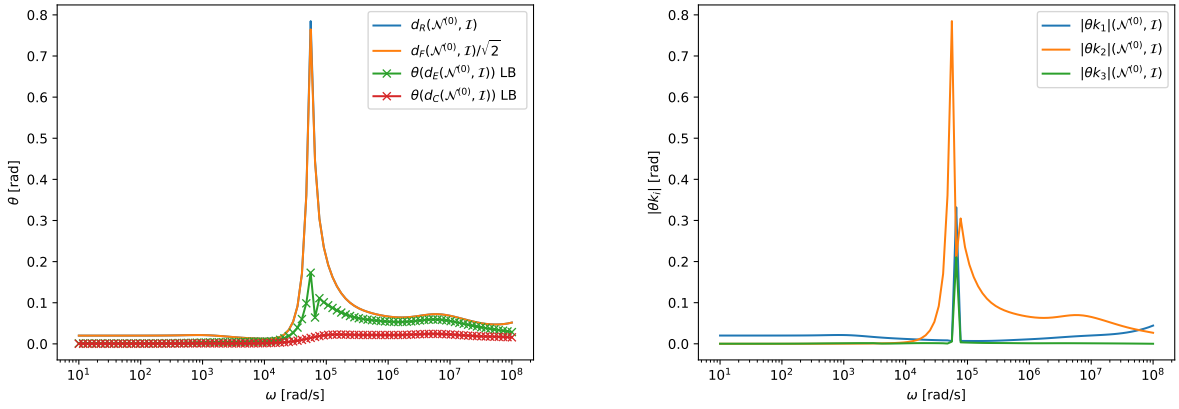

Figure 4: Toy gun with $\mu_r = 20$ in the barrel. Left: Angle measures $d_R(\mathcal{N}^{(0)}, \mathcal{I})$ and $d_F(\mathcal{N}^{(0)}, \mathcal{I})/\sqrt{2}$ using the eigenvectors and $\theta(d_E(\mathcal{N}^{(0)}, \mathcal{I})$ and $\theta(d_C(\mathcal{N}^{(0)}, \mathcal{I})$ without using the eigenvectors Right: Components of $|\theta k_i(\mathcal{N}^{(0)}, \mathcal{I})|$.

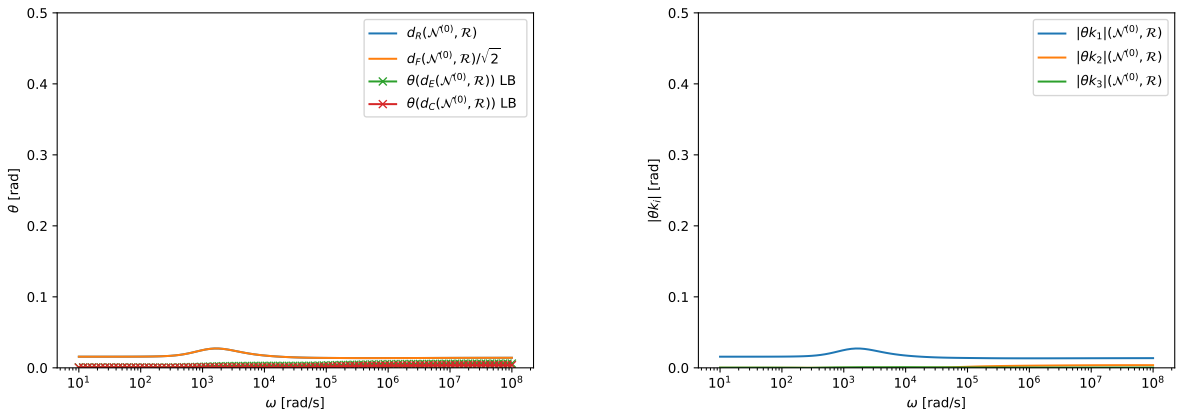

Figure 5: Toy gun with $\mu_r = 20$ in the barrel. Left: Angle measures $d_R(\mathcal{N}^{(0)}, \mathcal{R})$ and $d_F(\mathcal{N}^{(0)}, \mathcal{R})/\sqrt{2}$ using the eigenvectors and $\theta(d_E(\mathcal{N}^{(0)}, \mathcal{R})$ and $\theta(d_C(\mathcal{N}^{(0)}, \mathcal{R})$ without using the eigenvectors Right: Components of $|\theta k_i(\mathcal{N}^{(0)}, \mathcal{R})|$.

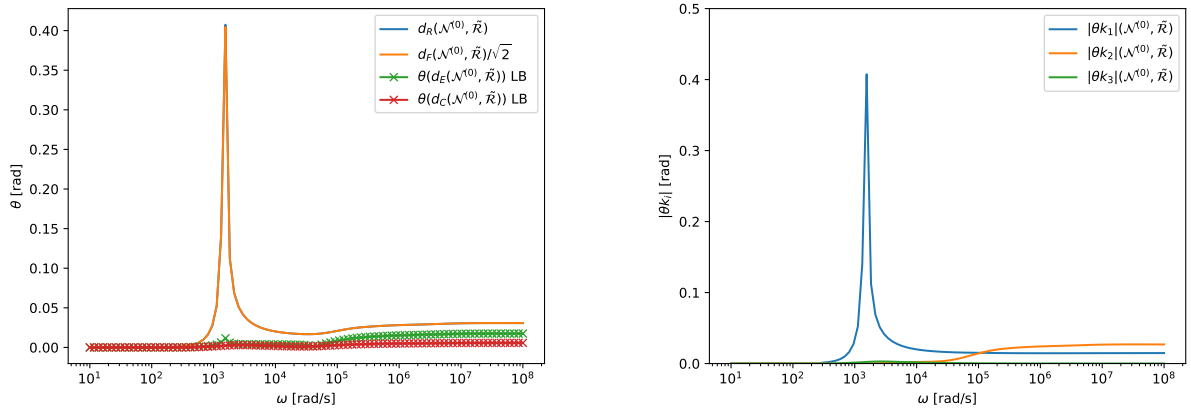

Figure 6: Toy gun with $\mu_r = 20$ in the barrel. Left: Angle measures $d_R(\mathcal{N}^{(0)}, \tilde{\mathcal{R}})$ and $d_F(\mathcal{N}^{(0)}, \tilde{\mathcal{R}})/\sqrt{2}$ using the eigenvectors and $\theta(d_E(\mathcal{N}^{(0)}, \tilde{\mathcal{R}})$ and $\theta(d_C(\mathcal{N}^{(0)}, \tilde{\mathcal{R}})$ without using the eigenvectors Right: Components of $|\theta k_i(\mathcal{N}^{(0)}, \tilde{\mathcal{R}})|$.

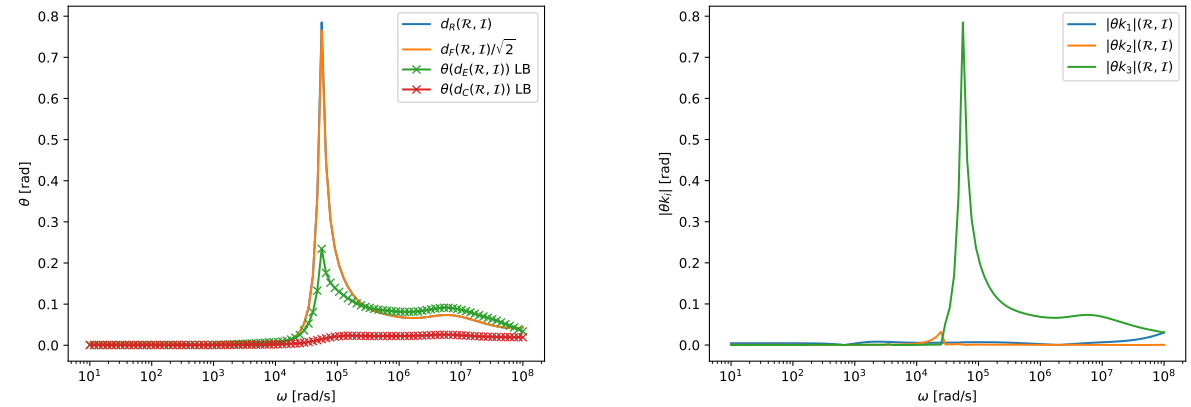

Figure 7: Toy gun with $\mu_r = 20$ in the barrel. Left: Angle measures $d_R(\mathcal{R}, \mathcal{I})$ and $d_F(\mathcal{R}, \mathcal{I})/\sqrt{2}$ using the eigenvectors and $\theta(d_E(\mathcal{R}, \mathcal{I})$ and $\theta(d_C(\mathcal{R}, \mathcal{I})$ without using the eigenvectors Right: Components of $|\theta k_i(\mathcal{R}, \mathcal{I})|$.

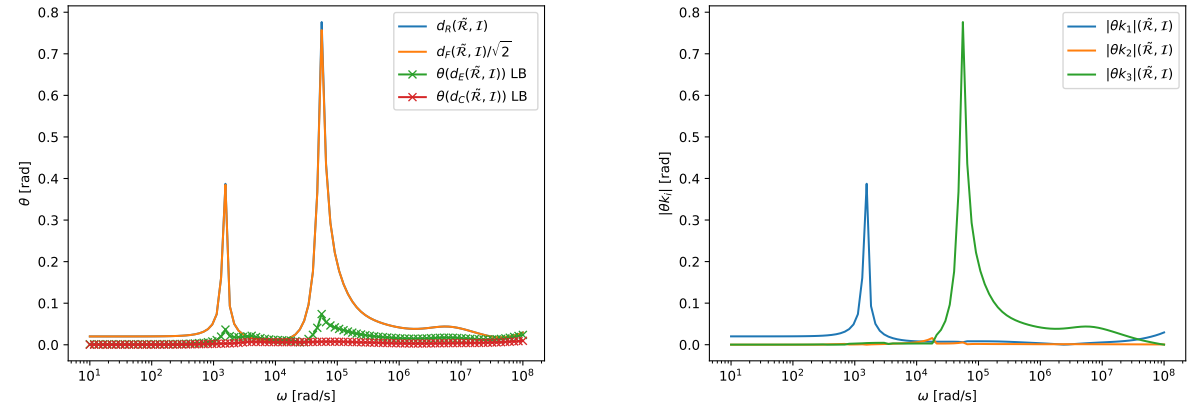

Figure 8: Toy gun with $\mu_r = 20$ in the barrel.Left:$d_R(\tilde{\mathcal{R}}, \mathcal{I})$ and $d_F(\tilde{\mathcal{R}}, \mathcal{I})/\sqrt{2}$ using the eigenvectors and $\theta(d_E(\tilde{\mathcal{R}}, \mathcal{I})$ and $\theta(d_C(\tilde{\mathcal{R}}, \mathcal{I})$ without using the eigenvectors.Right: Components of $|\theta k_i(\tilde{\mathcal{R}}, \mathcal{I})|$.

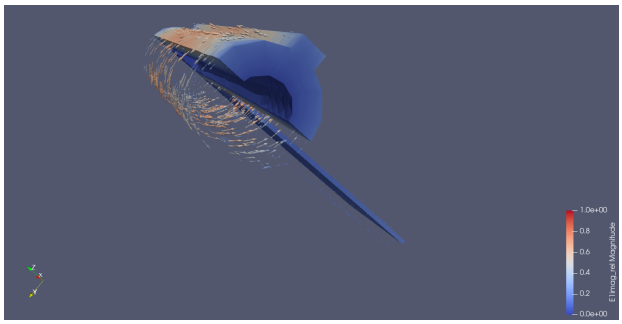

$\mathrm{Im}(\boldsymbol{J}_1)/|\mathrm{Im}(\boldsymbol{J}_1| = \mathrm{Im}(\mathrm{i}\omega\sigma_*\boldsymbol{\theta}_1^{(1)})/|\mathrm{Im}(\mathrm{i}\omega\sigma_*\boldsymbol{\theta}_1^{(1)})|$

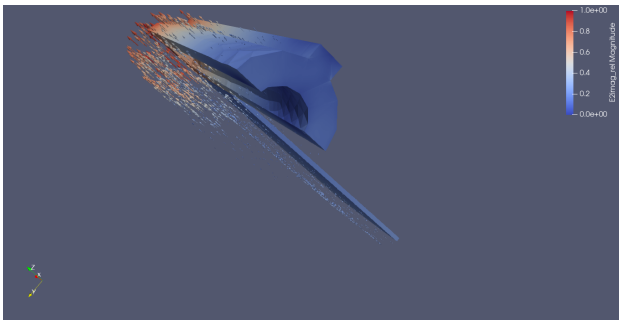

$\mathrm{Im}(\boldsymbol{J}_1)/|\mathrm{Im}(\boldsymbol{J}_1| = \mathrm{Im}(\mathrm{i}\omega\sigma_*\boldsymbol{\theta}_2^{(1)})/|\mathrm{Im}(\mathrm{i}\omega\sigma_*\boldsymbol{\theta}_2^{(1)})|$

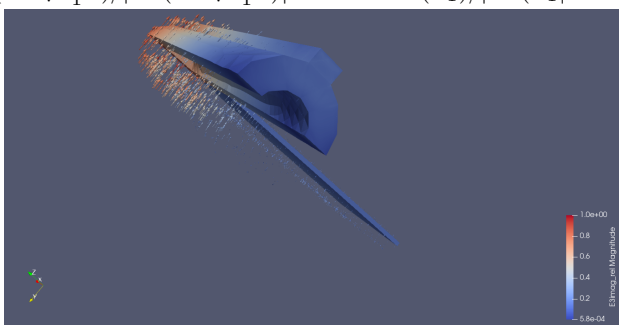

$\mathrm{Im}(\boldsymbol{J}_3)/|\mathrm{Im}(\boldsymbol{J}_3| = \mathrm{Im}(\mathrm{i}\omega\sigma_*\boldsymbol{\theta}_3^{(1)})/|\mathrm{Im}(\mathrm{i}\omega\sigma_*\boldsymbol{\theta}_3^{(1)})|$

Figure 9: Toy gun with $\mu_r = 20$ in the barrel. Normalised eddy current at $\omega = 7 \times 10^4$ rad/s

0.2 Barrel with $\mu_r = 100$

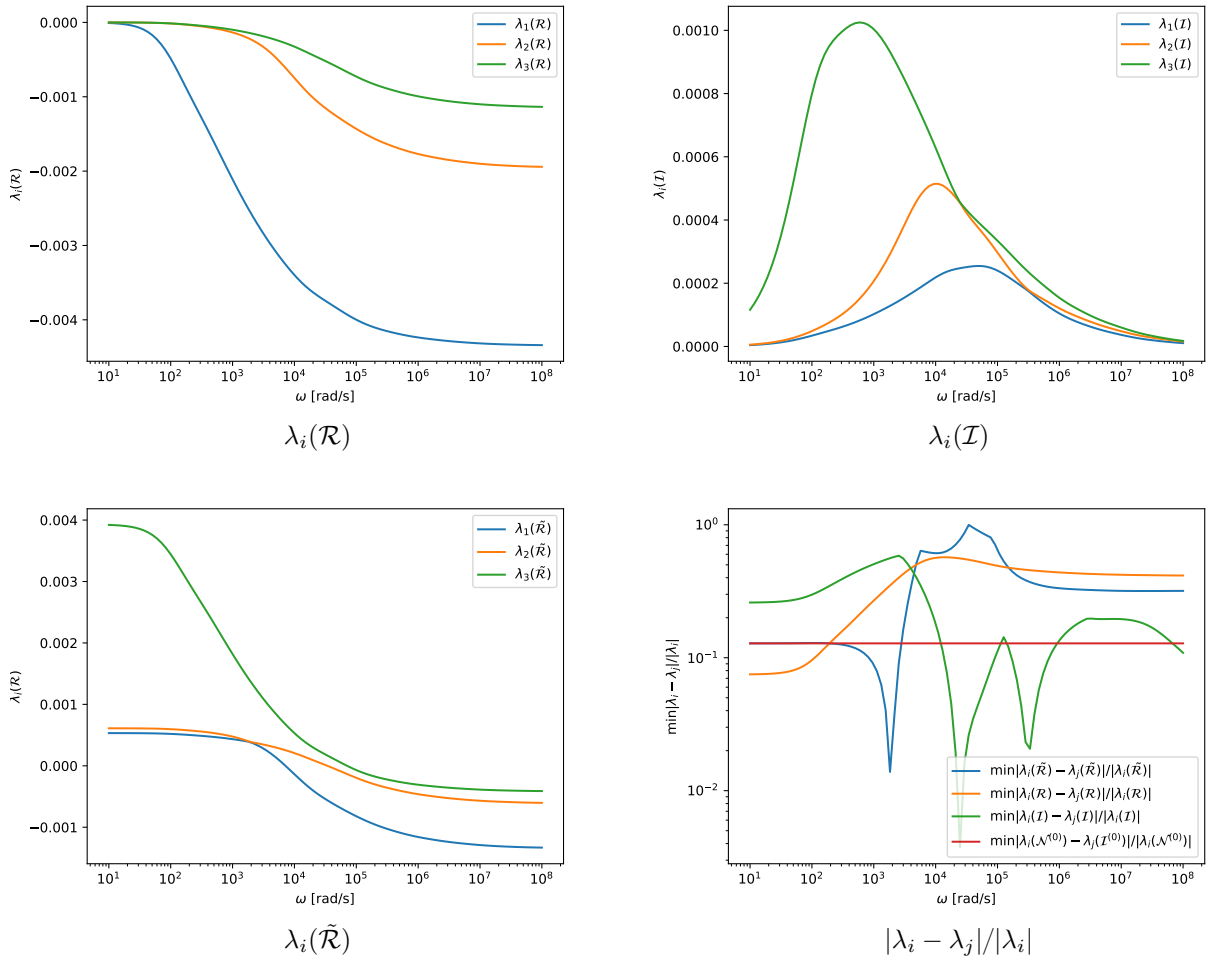

Figure 10: Computed $\lambda_n(\tilde{\mathcal{R}})$ (left) and $\lambda_n(\mathcal{I})$ (right) for the toy gun with $\mu_r = 100$ in the barrel. Notice that $\lambda_2(\mathcal{I}) = \lambda_3(\mathcal{I})$ for $\omega \approx 4 \times 10^4$ rad/s, $\lambda_1(\mathcal{I}) = \lambda_2(\mathcal{I})$ for $\omega \approx 6 \times 10^5$ rad/s and $\lambda_1(\tilde{\mathcal{R}}) \approx \lambda_2(\tilde{\mathcal{R}})$ for $\omega \approx 2 \times 10^3$ rad/s

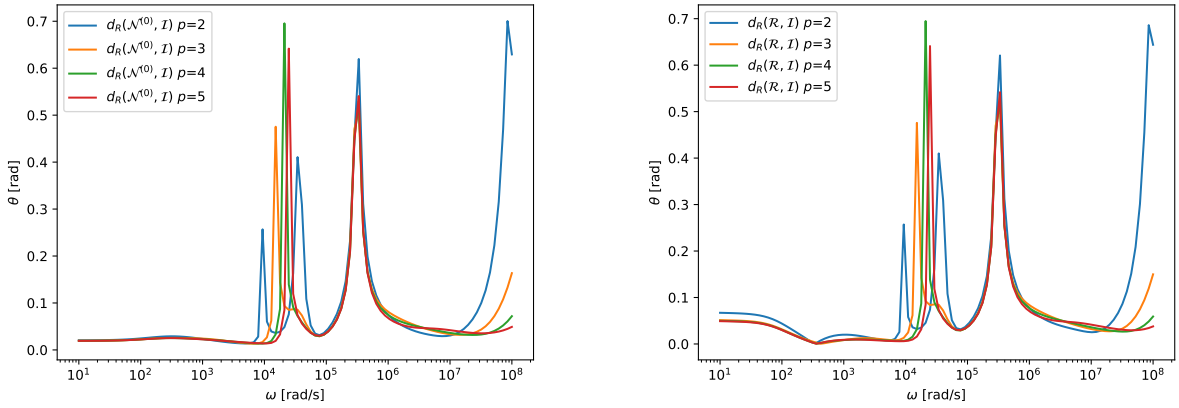

Figure 11: p refinement for the toy gun with $\mu_r = 100$ in the barrel. Angle measures $d_R(\mathcal{N}^{(0)}, \mathcal{I})$ and $d_R(\mathcal{R}, \mathcal{I})$

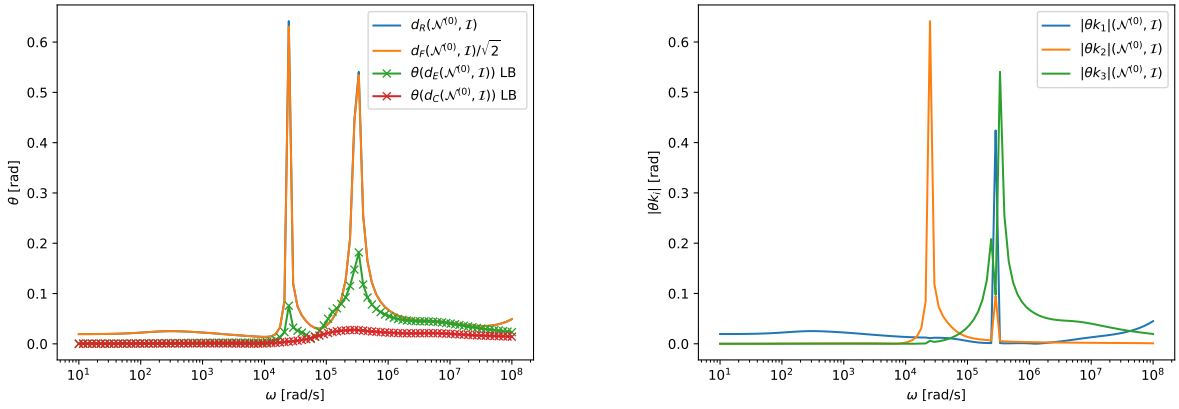

Figure 12: Toy gun with $\mu_r = 20$ in the barrel. Left: Angle measures $d_R(\mathcal{N}^{(0)}, \mathcal{I})$ and $d_F(\mathcal{N}^{(0)}, \mathcal{I})/\sqrt{2}$ using the eigenvectors and $\theta(d_E(\mathcal{N}^{(0)}, \mathcal{I})$ and $\theta(d_C(\mathcal{N}^{(0)}, \mathcal{I})$ without using the eigenvectors Right: Components of $|\theta k_i(\mathcal{N}^{(0)}, \mathcal{I})|$.

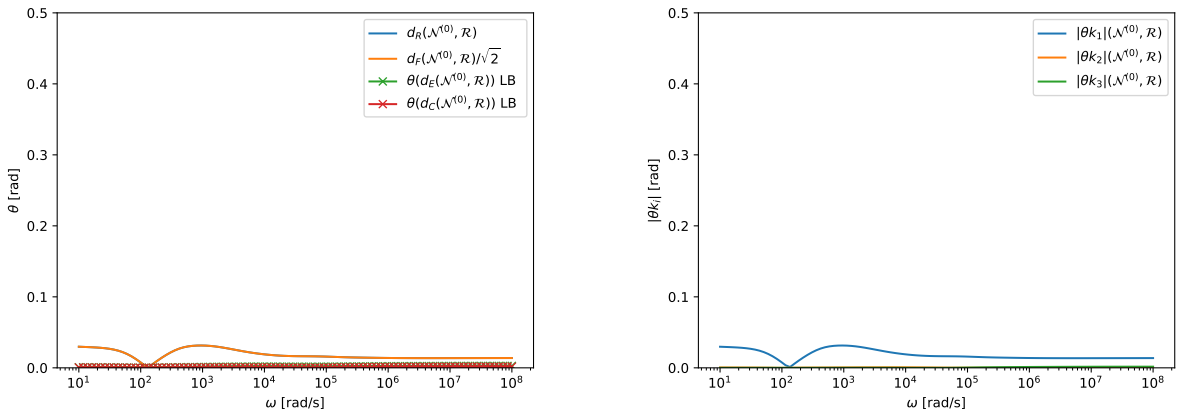

Figure 13: Toy gun with $\mu_r = 20$ in the barrel. Left: Angle measures $d_R(\mathcal{N}^{(0)}, \mathcal{R})$ and $d_F(\mathcal{N}^{(0)}, \mathcal{R})/\sqrt{2}$ using the eigenvectors and $\theta(d_E(\mathcal{N}^{(0)}, \mathcal{R})$ and $\theta(d_C(\mathcal{N}^{(0)}, \mathcal{R})$ without using the eigenvectors Right: Components of $|\theta k_i(\mathcal{N}^{(0)}, \mathcal{R})|$.

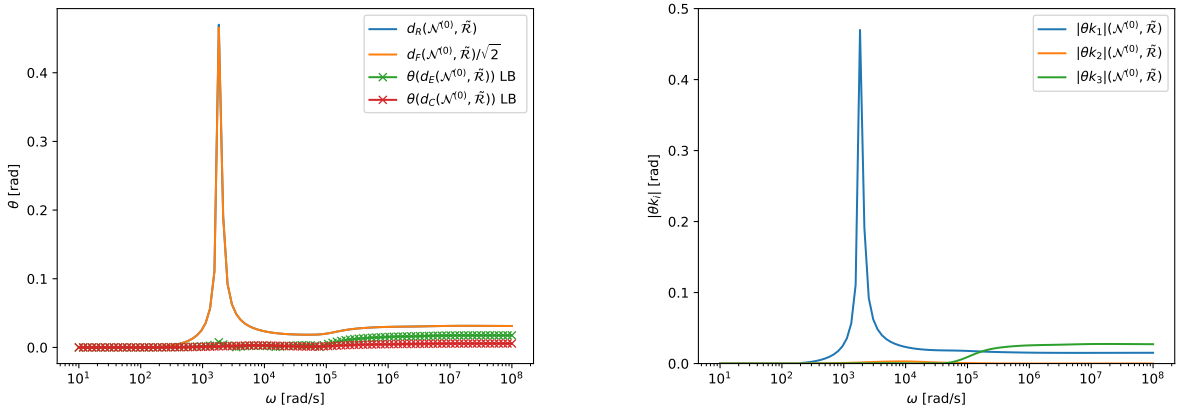

Figure 14: Toy gun with $\mu_r = 100$ in the barrel. Left: Angle measures $d_R(\mathcal{N}^{(0)}, \tilde{\mathcal{R}})$ and $d_F(\mathcal{N}^{(0)}, \tilde{\mathcal{R}})/\sqrt{2}$ using the eigenvectors and $\theta(d_E(\mathcal{N}^{(0)}, \tilde{\mathcal{R}})$ and $\theta(d_C(\mathcal{N}^{(0)}, \tilde{\mathcal{R}})$ without using the eigenvectors Right: Components of $|\theta k_i(\mathcal{N}^{(0)}, \tilde{\mathcal{R}})|$.

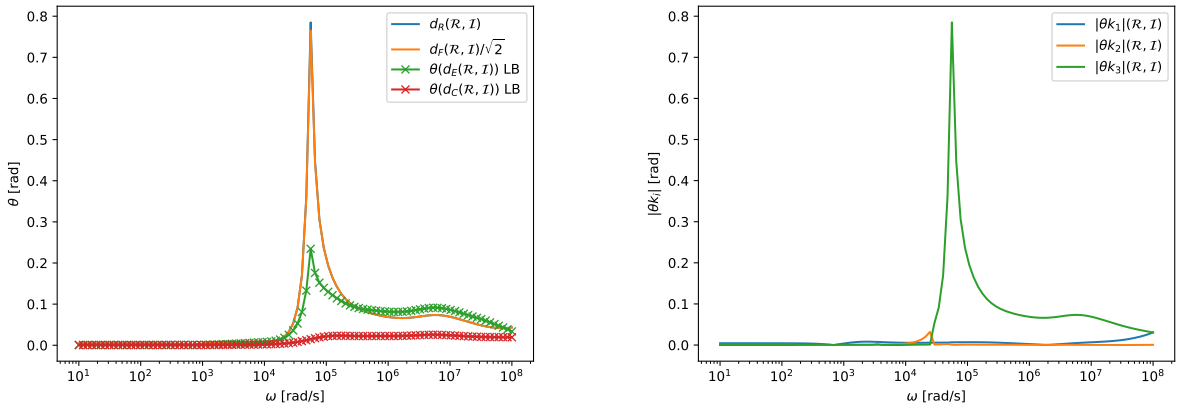

Figure 15: Toy gun with $\mu_r = 20$ in the barrel. Left: Angle measures $d_R(\mathcal{R}, \mathcal{I})$ and $d_F(\mathcal{R}, \mathcal{I})/\sqrt{2}$ using the eigenvectors and $\theta(d_E(\mathcal{R}, \mathcal{I})$ and $\theta(d_C(\mathcal{R}, \mathcal{I})$ without using the eigenvectors Right: Components of $|\theta k_i(\mathcal{R}, \mathcal{I})|$.

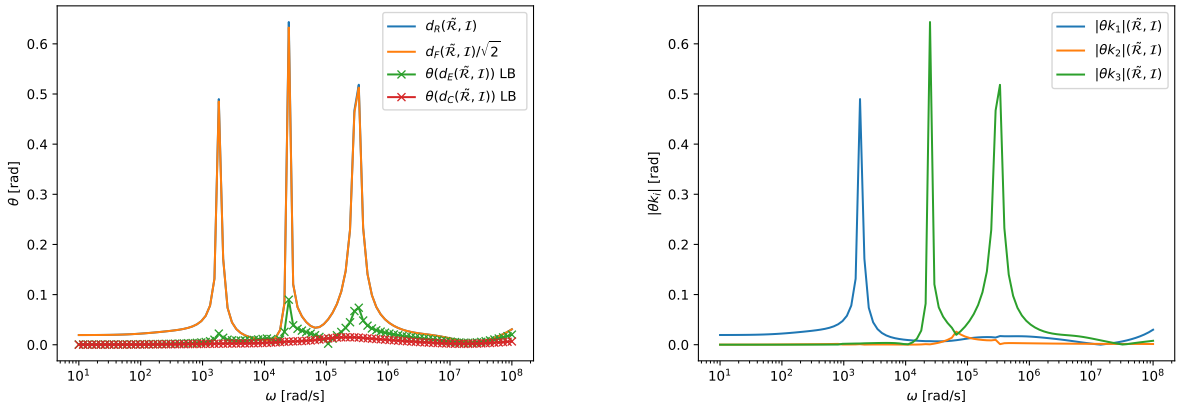

Figure 16: Toy gun with $\mu_r = 100$ in the barrel.Left:$d_R(\tilde{\mathcal{R}}, \mathcal{I})$ and $d_F(\tilde{\mathcal{R}}, \mathcal{I})/\sqrt{2}$ using the eigenvectors and $\theta(d_E(\tilde{\mathcal{R}}, \mathcal{I})$ and $\theta(d_C(\tilde{\mathcal{R}}, \mathcal{I})$ without using the eigenvectors.Right: Components of $|\theta k_i(\tilde{\mathcal{R}}, \mathcal{I})|$.